itance, which is the sum of depletion capacitances and the oxide capacitance is between 1 and 2×10^5 pF/cm^2. From the results obtained the total capacitance of an optimised device structure ($l_g = 1\,\mu$m, $w_g = 30\,\mu$m) is calculated to be ~ 30 fF which is small enough for applications up to 10 Gbit/s.

To test the devices a microwave setup (rise time 25 ps) was used. The devices were characterised in the triggered travelling domain mode. Single domains were triggered by gate pulses of 0·5 V and of 200 ps duration (full width at half maximum (FWHM)). The triggered current drops were 35 mA, equivalent to 55%. For the tested device the FWHM of the current drops was 260 ps which corresponds closely to the length of 30 μm between gate and anode. For shorter devices switching times of less than 100 ps could be achieved. The measured rise and fall times were 50 ps including the rise time of the experimental setup. The transconductance of the devices below the Gunn threshold was ~ 10 mS/mm which results from the large gate length ($\sim 10\,\mu$m) and from the low electron concentration of the InGaAs layer. However, optimising these parameters should lead to higher transconductances by an order of magnitude for 1 μm long gates and an improved trigger sensitivity of the devices.

Conclusion: In summary, we demonstrate for the first time the triggering of single domains in InGaAs-transferred-electron devices having a MESFET-like structure. Current drops of 35 mA with an FWHM of 260 ps were triggered by 0·5 V pulses. We tested several enhancement layers to increase the Schottky barrier height on InGaAs which is essential for the realisation of the gate electrode. Barrier heights between 0·53 and 0·67 eV were obtained. The quasi-Schottky-diodes employed as gates had reverse current densities of 10^{-3} A/cm^2 at -1 V. Further improvements in the devices can be expected by reducing the gate length and increasing the doping concentration of the InGaAs layer. From the results which were measured with actual devices (and not with large area diodes as is usually done) it can be expected that the devices can be used advantageously for high-speed applications in InP-based integrated circuits or as simple millimetre wave oscillators.

Acknowledgment: The authors would like to thank H. Newi and D. Rümmler for their contributions to the experimental work and L. Malacky for stimulating discussions. This work was financially supported by the DBP Telekom.

4th May 1993

D. Hahn, G. Zwinge and A. Schlachetzki (*Institut für Halbleitertechnik, Technical University Braunschweig, D-W-3300 Braunschweig Germany*)

References

1 KOWALSKY, W., and SCHLACHETZKI, A.: 'Analysis of the transferred-electron effect in the InGaAsP system', *Solid-State Electron.*, 1987, **30**, pp. 161–172

2 HAHN, D., HANSEN, K., and SCHLACHETZKI, A.: 'Experimental study of InGaAs transferred electron device as fast laser driver', *Electron. Lett.*, 1991, **27**, pp. 2070–2072

3 LUGLI, P., GRIMM, M., PABST, M., and LÜTH, H.: 'Travelling Gunn domains in submicron GaAs MESFETs', *Electron. Lett.*, 1991, **27**, pp. 398–400

4 DISKUS, C. G., LÜBKE, K., SPRINGER, A. L., LETTENMAYR, H. W., and THIM, H. W.:'Gunn effect in MESFET like structures', *Electron. Lett.*, 1992, **28**, pp. 980–981

5 KORDOŠ, P., MARSO, M., MEYER, R., and LÜTH, H.: 'Schottky barrier enhancement on n-$In_{0.53}Ga_{0.47}As$', *J. Appl. Phys.*, 1992, **72**, pp. 2347–2355

6 SUGETA, T., TANIMOTO, M., IKOMA, T., and YANAI, H.: 'Characteristics and applications of a Schottky-barrier-gate Gunn-effect digital device', *IEEE Trans.*, 1974, **ED-21**, pp. 504–515

7 SZE, S. M.: 'Physics of semiconductor devices' (John Wiley & Sons Inc., New York, 1981)

8 HO, M. C., HE, Y., CHIN, T. P., LIANG, B. W., and TU, C. W.: 'Enhancement of effective Schottky barrier height on *n*-type InP', *Electron. Lett.*, 1992, **28**, pp. 68–71

9 BÖTTCHER, E. H., KUHL, D., HIERONYMI, F., DRÖGE, E., WOLF, T., and BIMBERG, D.: 'Ultrafast semiinsulating InP : Fe-InGaAs : Fe-InP : Fe MSM photodetectors: Modelling and performance', *IEEE J. Quantum Electron.*, 1992, **QE-28**, pp. 2343–2357

JAKES FADING MODEL REVISITED

P. Dent, G. E. Bottomley and T. Croft

Indexing terms: Fading, Mobile radio systems

With the popular Jakes fading model, it is difficult to create multiple uncorrelated fading waveforms. In the Letter, modifications to the model are proposed which solve this problem.

Introduction: The Jakes fading model is a deterministic method for simulating time-correlated Rayleigh fading waveforms [1] and is still widely used today [2–4]. The model assumes that N equal-strength rays arrive at a moving receiver with uniformly distributed arrival angles α_n, such that ray n experiences a Doppler shift $\omega_n = \omega_M \cos(\alpha_n)$, where $\omega_M = 2\pi f v/c$ is the maximum Doppler shift, v is the vehicle speed, f is the carrier frequency, and c is the speed of light.

Using $\alpha_n = 2\pi n/N$ [1] (see Fig. 1), there is quadrantal symmetry in the magnitude of the Doppler shift, except for angles

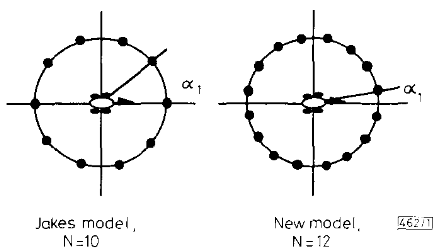

Fig. 1 *Ray arrival angles in Jakes (N = 10) and new models (N = 12)*

0 and π. As a result, the fading waveform can be modelled with $N_0 + 1$ complex oscillators, where $N_0 = (N/2 - 1)/2$. This gives

$$T(t) = K\left\{\frac{1}{\sqrt{(2)}}[\cos(\alpha) + I\sin(\alpha)]\cos(\omega_M t + \theta_0) + \sum_{n=1}^{N_0}[\cos(\beta_n) + I\sin(\beta_n)]\cos(\omega_n t + \theta_n)\right\} \quad (1)$$

where I denotes $\sqrt{(-1)}$ (j is used in Reference 1 for waveform index), K is a normalisation constant, α (not the same as α_n) and β_n are phases, and θ_n are initial phases usually set to zero. Setting $\alpha = 0$ and $\beta_n = \pi n/(N_0 + 1)$ gives zero crosscorrelation between the real and imaginary parts of $T(t)$.

To generate multiple uncorrelated waveforms, Jakes [1] suggests using phases $\theta_{n,j} = \beta_n + 2\pi(j - 1)/(N_0 + 1)$, where $j = 1$ to N_0 is the waveform index. However, this gives almost uncorrelated waveforms j and k only when $\theta_{n,j} - \theta_{n,k} = i\pi + \pi/2$, for some integer i. Otherwise, the correlation between certain waveform pairs can be significant [5].

In this Letter, a remedy for this problem is proposed in which orthogonal functions (Walsh–Hadamard codewords) weight the oscillator values before summing. To eliminate correlation, the oscillators must have equal power. This is achieved by reformulating the Jakes model in terms of slightly different arrival angles.

Model reformulation: To provide quadrantal symmetry for *all* Doppler shifts, which leads to equal power oscillators, the following arrival angles are used (see Fig. 1): $\alpha_n = 2\pi(n - 0.5)/N$. Following the procedure in Reference 1, this leads to the model

$$T(t) = \sqrt{\left(\frac{2}{N_0}\right)}\sum_{n=1}^{N_0}[\cos(\beta_n) + I\sin(\beta_n)]\cos(\omega_n t + \theta_n) \quad (2)$$

where $N_0 = N/4$ and the normalisation factor $\sqrt{(2/N_0)}$ gives $E\{T(t)T^*(t)\} = 1$. Moment and correlation expressions are similar to those in Reference 1, with the absence of the terms depending on α.

By using $\beta_n = \pi n/N_0$, the real and imaginary parts of $T(t)$

have equal power and are uncorrelated. Randomising θ_n provides different waveform realisations.

Multiple uncorrelated waveforms: Many application simulations require multiple uncorrelated waveforms. Waveform crosscorrelation is determined by the sum of the product of the oscillator coefficients, which can be viewed as a vector inner product. Orthogonal vectors, such as Walsh–Hadamard (WH) codewords [6], give zero inner product values with one another. Thus, with N_0 a power of two, the jth waveform can be generated using

$$T(t, j) = \sqrt{\left(\frac{2}{N_0}\right)} \sum_{n=1}^{N_0} A_j(n) \times \{[\cos(\beta_n) + I \sin(\beta_n)] \cos(\omega_n t + \theta_n)\} \quad (3)$$

where $A_j(n)$ is the jth WH code sequence in n (± 1 values). This gives N_0 uncorrelated waveforms, which can be efficiently generated by passing the original N_0 complex oscillator values through a fast Walsh transform (FWT). Correlation properties are insensitive to the random number seed used to initialise the oscillator phases θ_n.

To obtain fewer waveforms, N_w a power of two and less than N_0, groups of N_0/N_w complex oscillators can be pre-summed before being passed through an N_w-point FWT. It is recommended that the pre-sums draw evenly from the Doppler spectrum, e.g. 1 + 5 + 9 + 13, 2 + 6 + 10 + 14, etc. for $N_0 = 16$, $N_w = 4$. This corresponds to the first stages of a decimate-in-frequency form FWT. Thus, if such an FWT is used after pre-summing, the same fading waveforms will be reproduced should less pre-summing be used in another simulation run.

Numerical results: A simulation was run to generate four uncorrelated complex baseband fading waveforms using $N_0 = 16$ oscillators. With a Doppler frequency $\omega_M = 2\pi(83)$, 1000000 samples of each fading waveform were generated using a sampling period of 383·5 μs. For each waveform, both autocorrelation (see Fig. 2) and probability density functions agreed well with theory.

Various moments and correlation coefficient values (ρ as defined in Reference 7) are compared to theoretical values in Table 1. Complex correlation coefficients between pairs of waveforms are given in Table 2. These results indicate good model performance.

Conclusion: The Jakes fading model provides multiple time correlated fading waveforms, but the waveforms are not truly uncorrelated with one another. By reformulating the model with slightly different ray arrival angles, N_0 equal-strength oscillators result, which can then be weighted by orthogonal weighting functions, such as Walsh–Hadamard sequences, to give up to N_0 uncorrelated fading waveforms. Simulation tests confirm that the new model produces uncorrelated fading waveforms whose behaviour matches theoretical expectations.

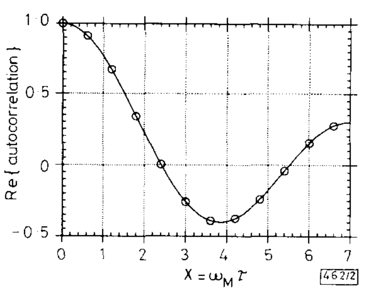

Fig. 2 *Autocorrelation function: simulated and theoretical results*
—— theory: $J_0(X)$
○ simulated

Table 2 MEASURED CORRELATION COEFFICIENTS BETWEEN WAVEFORMS

Wave (j)	Wave (k)	Crosscorrelation ($\rho\{T(t, j), T^*(t, k)\}$)
0	1	$-4.7 \times 10^{-5} + i(2.1 \times 10^{-5})$
0	2	$-4.0 \times 10^{-6} + i(2.8 \times 10^{-5})$
0	3	$-3.2 \times 10^{-5} - i(7.0 \times 10^{-6})$
1	2	$3.4 \times 10^{-5} - i(4.0 \times 10^{-6})$
1	3	$-1.5 \times 10^{-5} - i(2.3 \times 10^{-5})$
2	3	$2.1 \times 10^{-5} - i(1.0 \times 10^{-5})$

Acknowledgments: The authors would like to thank S. Chennakeshu, B. Gudmundson, and J. C. Chen for their helpful comments and suggestions.

23rd March 1993

P. Dent, G. E. Bottomley and T. Croft (*Ericsson GE Mobile Communications, Inc., 1 Triangle Drive, PO Box 13969, RTP, NC, USA*)

References

1 JAKES, W. C., JUN. (Ed.): 'Microwave mobile communications' (Wiley, New York, 1974)
2 KOILPILLAI, R. D., CHENNAKESHU, S., and TOY, R. T.: 'Low complexity equalizers for U.S. digital cellular system'. Proc. VTC '92, Denver, CO, 10th–13th May 1992
3 LO, N. W. K., FALCONER, D. D., and SHEIKH, A. U. H.: 'Adaptive equalization and diversity combining for mobile radio using interpolated channel estimates', *IEEE Trans.*, 1991, **VT-40**, (3), pp. 636–645
4 STÜBER, G. L., and YIIN, L.-B.: 'Downlink outage predictions for cellular radio systems', *IEEE Trans.*, 1991, **VT-40**, (3), pp. 521–531
5 VON ECKARDSTEIN, S., and ISAKSSON, K.: 'Kanalmodeller för radiotransmission (Channel models for radio transmission)'. Master's Thesis, Royal Institute of Technology, Stockholm, Sweden, December 1991 (in Swedish)
6 AHMED, N., and RAO, K. R.: 'Orthogonal transforms for digital signal processing' (Springer-Verlag, New York, 1975)
7 PAPOULIS, A.: 'Probability, random variables, and stochastic processes' (McGraw-Hill, New York, 1965)

WAVELENGTH-INSENSITIVE FUSED POLISHED COUPLERS

C. V. Cryan, K. P. Oakley and C. D. Hussey

Indexing terms: Optical couplers, Optical fibres

Wavelength-insensitive fused polished couplers are fabricated both from different fibres and from identical fibres where in the latter case one of the fibres is polished to such an extent that a small portion of its core is removed.

Introduction: The production of a wavelength-insensitive response in fused tapered couplers by inducing an asymmetry

Table 1 FADING PROCESS MOMENTS: SIMULATED AND THEORETICAL VALUES

Moment	Ideal	Wave 0	Wave 1	Wave 2	Wave 3
$\mathrm{Re}\{E\{T(t, j)\}\}$	0·0	-1.297×10^{-5}	-1.446×10^{-5}	2.064×10^{-5}	2.489×10^{-5}
$\mathrm{Im}\{E\{T(t, j)\}\}$	0·0	-1.030×10^{-5}	-2.0×10^{-7}	-8.39×10^{-6}	-5.36×10^{-6}
$E\{\mathrm{Re}\{T(t, j)\}^2\}$	0·5	0·499827	0·499710	0·499772	0·499813
$E\{\mathrm{Im}\{T(t, j)\}^2\}$	0·5	0·499825	0·499722	0·499755	0·499770
$\rho\{\mathrm{Re}\{T(t, j)\}, \mathrm{Im}\{T(t, j)\}\}$	0·0	5.793×10^{-5}	-9.206×10^{-5}	-8.38×10^{-6}	-1.056×10^{-5}
$\mathrm{Re}\{E\{T(t, j), T^*(t, j)\}\}$	1·0	0·999985	0·999807	0·999880	0·999907